Close Contacts and Noncovalent Interactions in Crystals

Jane S. Murray,[a] Guiseppe Resnati[b] and Peter Politzer[a]

[a]Department of Chemistry, University of New Orleans, New Orleans, LA 70148 USA.

[b]Laboratory of Nanostructured Fluorinated Materials (NFMLab), Department of Chemistry, Materials, and Chemical Engineering "Giulio Natta," Politecnico di Milano, Via L. Mancinelli 7, 20131 Milano, Italy.

1. Close Contacts in Crystal Lattices

Attractive noncovalent interactions within crystal lattices are typically identified by finding close contacts between atoms. A close contact is usually defined as a separation that is less than the sum of the van der Waals radii of the respective atoms. This is a widely used and seemingly reasonable approach, and has indeed played a key role in establishing the existence of halogen bonding[1-3] as well as analogous interactions involving atoms of other Groups.[4-7] However there are at least two problems associated with identifying noncovalent interactions in this manner.

First is the issue of determining and interpreting van der Waals radii. Various methods have been used to assign their values. Pauling based them on the radii of the corresponding negative ions,[8] but warned that they "are to be considered as reliable only to 0.05 or 0.10 Å." Bondi's radii have been invoked very extensively in relation to close contacts, but he similarly gave a warning:[9] "It cannot be overemphasized that the van der Waals radii of this paper have been selected for the calculation of volumes. They may not always be suitable for the calculation of contact distances in crystals." He also recognized that assuming atoms in molecules to be spherical is not valid, a point that was stressed as well by Nyburg and Faerman,[10] who further noted that the van der Waals radius of an atom should be expected to be affected by its molecular environment. More recent compilations of van der Waals radii have involved surveying of crystal structures to tabulate the separations between given pairs of atoms, then identifying a range corresponding to nonbonded interactions and selecting on some basis an intermediate value within this range to statistically apportion between each pair of atoms.[11-13]

While the results of these various approaches are overall similar – perhaps surprisingly so – there can be significant differences. Thus Bondi's value for sulfur is 1.80 Å,[9] whereas Alvarez gives it as 1.89 Å.[13] More important, using an intermediate separation to establish the atoms' radii means that some nonbonded interactions are necessarily at distances greater than the van der Waals sum. Dance[12] and Alvarez[13] have pointed out that separations exceeding this sum by several tenths of an Ångstrom can still correspond to attractive interactions.

These comments are not meant to deny the usefulness of van der Waals radii as a *rough* guide to noncovalent interactions. But it might be well to follow Pauling's lead and give their sums to only one decimal place, and not to view these sums as a rigorous criterion for a noncovalent interaction.

A second problem relating to the use of interatomic close contacts to identify attractive noncovalent interactions is that it may be misleading, in some instances, to attribute these interactions to specific atoms. This is the subject of the present paper.

2. σ-Holes: The Halogens and Hydrogen

Halogen atoms normally form only a single covalent bond, and therefore often protrude from the remainder of the molecule. This facilitates the recognition and analysis of their noncovalent interactions, since they are less likely to be affected or obscured by neighboring portions of the molecule than are those of atoms that form two or more covalent bonds.

Of particular interest in recent years have been the noncovalent interactions of many covalently-bonded halogen atoms with negative sites. This known as halogen bonding. It was long regarded as enigmatic, because the halogen is the most electronegative atom in each row of the periodic table and hence would not be expected to interact attractively with a negative site. This issue was resolved by the rather surprising discovery that many covalently-bonded halogen atoms have regions of positive electrostatic potential on their outer sides, along the extensions of their covalent bonds,[14,15] while their lateral sides are negative. This explained what Murray-Rust et al had found through crystallographic surveys of organic halides:[1-3] Close contacts between the halogen atoms and nucleophilic sites are approximately along the extensions of the C-X bonds (X = Cl, Br, I), while close contacts with electrophilic sites involve the halogens' lateral sides.

The origin of the unexpected outer positive regions lies in the anisotropies of the charge distributions of covalently-bonded halogen atoms. The charge rearrangement that accompanies

the bond formation typically results in there being less electronic density on the extension of the bond than on the atom's lateral sides.[16-21] For the less electronegative iodine and bromine, the outer region usually has a positive electrostatic potential, while the lateral sides are negative. This is often true for chlorine as well. Thus the atom can undergo attractive interactions with negative sites through its positive outer region and with positive sites through its lateral sides.[22]

Clark proposed the term "σ-hole" for the region of lesser electronic density on the extension of the covalent σ bond to a halogen.[23] σ-Holes sometimes have negative electrostatic potentials, but even then they are less negative than the surrounding region. Fluorine, the most electronegative halogen, often has a negative σ-hole, although it can have a positive one when the remainder of the molecule is sufficiently electron-attracting.[24-28]

Hydrogen bonding is also a σ-hole interaction;[29-31] a covalently-bonded hydrogen clearly has less electronic density on its outer side since its only electron is involved in the bond. A hydrogen σ-hole is in fact approximately hemispherical and thus less focused than is that of a halogen.[32] As a result, hydrogen bonding is in general more likely to deviate from linearity than is halogen bonding.[32-34]

The similarities and differences between halogen and hydrogen σ-holes are illustrated in Figure 1, which shows the computed electrostatic potential on the molecular surface of 4-bromo-2*H*-1,2,3-triazole, **1**. The molecular surface is taken to be the 0.001 au contour of the molecule's electronic density, as suggested by Bader et al.[35] The calculations were at the density functional M06-2X/6-311G(d) level, and the electrostatic potential was obtained with the WFA-SAS code.[36]

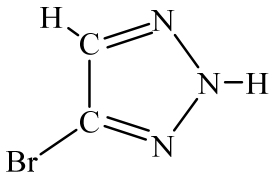

1

Figure 1 clearly shows the bromine protruding from the heterocyclic ring of **1**. There are three regions of positive electrostatic potential, one on the bromine and two on the hydrogens. They correspond to σ-holes on the extensions of the C-Br, N-H and C-H bonds. Their most positive values, designated by the label $V_{S,max}$, are all located very close to the extensions of the respective bonds, within $2^o - 4^o$. The most positive $V_{S,max}$ is on the N-H hydrogen, reflecting the electronegativity of the nitrogen; its magnitude is 58 kcal/mol. The $V_{S,max}$ of the other hydrogen is 26 kcal/mole, while that of the bromine is 18 kcal/mol. As mentioned earlier, the σ-hole positive potentials of the hydrogens extend over hemispherical surfaces whereas that of the bromine is more narrowly focused along the extension of the C-Br bond, with the lateral sides of the bromine being completely negative. It follows that the interaction of the bromine with a negative site B is more likely to be nearly linear (the C-Br---B angle being approximately 180^o) than are analogous interactions of the hydrogens, which can occur over a wider range of angles.

3. σ-Holes: Groups IV−VI

Like the halogens and hydrogen, covalently-bonded atoms of Groups IV – VI also have σ-holes, i.e. regions of less electronic density on the extensions of the bonds.[5,6,37,38] When these give rise to positive electrostatic potentials, they can again result in attractive interactions with negative sites.[4-7,22]

However the electrostatic potentials on the surfaces of the Group IV –VI atoms are likely to be somewhat less straightforward than those of the halogens and hydrogen. It is important to recognize that whereas the electronic density at a point **r** is a measure of the amount of electronic charge at just that **r**, the electrostatic potential at the same **r** is the resultant of the potentials exerted at **r** by all of the nuclei and electronic charge elements of the entire molecule.[39-41] For the Group IV – VI atoms, which often have neighbors in close proximity, both the magnitudes and the locations of the potentials due to their σ-holes may be significantly affected by the electrostatic potentials of these neighbors.

Consider the molecule cyanodimethylarsine, **2**. In Figure 2 is the computed electrostatic potential on its 0.001 au surface. Note that much of the arsenic surface is positive; only its localized lone pair produces a negative potential. The arsenic σ-hole resulting from the bond to the electron-attracting cyano group can be expected to have a strongly-positive potential, but it overlaps and is reinforced by those of the σ-holes of the two nearby methyl hydrogens, Figure 2(a). This results in an extended positive region with just a single $V_{S,max}$, 34 kcal/mol, even though it reflects three σ-holes. The overlap also shifts the position of this $V_{S,max}$ by about 21° away from the extension of the NC-As bond.

The positive potentials of the arsenic σ-holes produced by the H_3C-As bonds are weaker, in part because methyl groups are less electron-attracting but also because of overlap with the lone pair negative potential, Figure 2(b). This causes their $V_{S,max}$, 20 kcal/mol, to deviate by about 21° from the extensions of the H_3C-As bonds. The four remaining hydrogens have similar $V_{S,max}$ of 20 kcal/mol but overlapping of positive regions leads to two of these being 37° and 41° from the extensions of the C-H bonds.

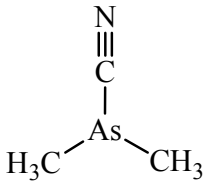

2

This example demonstrates the complexity that may be associated with the surface electrostatic potential of even a relatively small molecule. Some degree of symmetry can help to reduce this complexity.

For instance, cyanotrimethylgermane, **3**, has a three-fold axis of symmetry, coinciding with the NC-Ge bond. The positive potential of the σ-hole on the extension of this bond does overlap those of methyl hydrogens but the symmetrical placement of the latter puts the single $V_{S,}$max, 34 kcal/mol, on the extension of the NC-Ge bond, Figure 3(a). The other germanium σ-holes have

$V_{S,max}$ that are very close to the extensions of the H_3C-Ge bonds, within 3° to 5°, Figure 3(b). Note that the germanium in **3** is entirely positive, as is usual for tetrahedral Group IV atoms.[42]

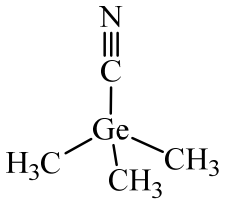

3

Our final example, involving a Group VI atom, is dicyanotelluride, **4**. Its electrostatic potential, reported elsewhere,[43] shows two strongly positive potentials with $V_{S,max}$ of 50 kcal/mol that can be attributed to tellurium σ-holes. The $V_{S,max}$ deviate by 17° from the extensions of the NC-Te bonds, which probably reflects some overlap of the potentials of the tellurium σ-holes and the carbons, which are completely positive. The tellurium surface is also entirely positive, even its lone pair region.

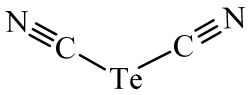

4

4. Close Contacts and Noncovalent Interactions

Numerous crystallographic studies of crystals and co-crystals based upon halogen bonding identified close contacts between halogen atoms and basic sites.[1-3,44-49] These close contacts are now known to correspond to Coulombic σ-hole interactions that control the crystal structures. Do close contacts also represent σ-hole interactions for Group IV−VI systems?

We shall consider first the crystalline forms of **2** − **4**, for which the molecular electrostatic potentials have been discussed above. The lattice structure of cyanodimethylarsine, **2**, was found[50] to consist of chains of molecules with intermolecular As---N close contacts, as depicted

in **5**. These close contacts can now be identified as interactions between the negative potentials of the cyano nitrogen lone pairs, Figure 2(b), and the extended positive regions arising from the overlapping arsenic and hydrogen σ-hole potentials, Figure 2(a). The $V_{S,max}$ of these positive regions are displaced by 21° from the extensions of the NC-As bonds, as mentioned in section 3, which can account for the chain of molecules being somewhat non-linear, as indicated in **5**.

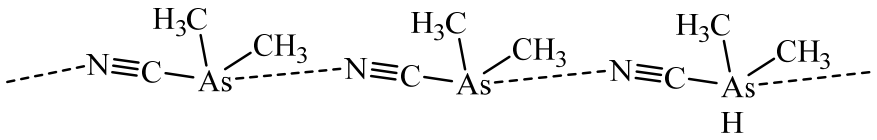

5

In contrast, the crystal lattice of cyanotrimethylgermane, **3**, has chains of molecules that are linear,[51] "with the cyanide group in one molecule pointing directly toward the germanium atom in the next." This is shown in **6**. These Ge---N close contacts correspond to the nitrogen lone pairs, Figure 3(b), interacting with the positive regions of the overlapping germanium and hydrogen σ-hole potentials, Figure 3(a). Since the $V_{S,max}$ of these positive regions are on the extensions of the NC-Ge bonds, the chain is linear, **6**.

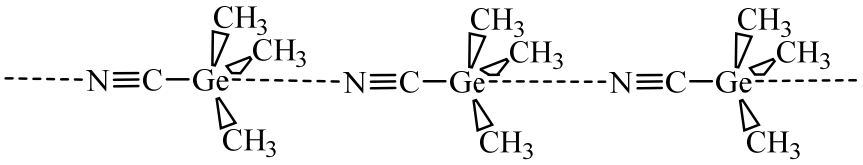

6

In the crystal lattice of **4**,[52] there is a network of $Te(CN)_2$ molecules linked by Te---N close contacts, as depicted in **7**. These can be interpreted as interactions between the positive σ-hole potentials of the telluriums and the nitrogen lone pair negative potentials. The C-Te---N angles are 163.2° and 163.3°, remarkably consistent with the observation in section 3 that the tellurium $V_{S,max}$ diverge by 17° from the extensions of the NC-Te bonds.

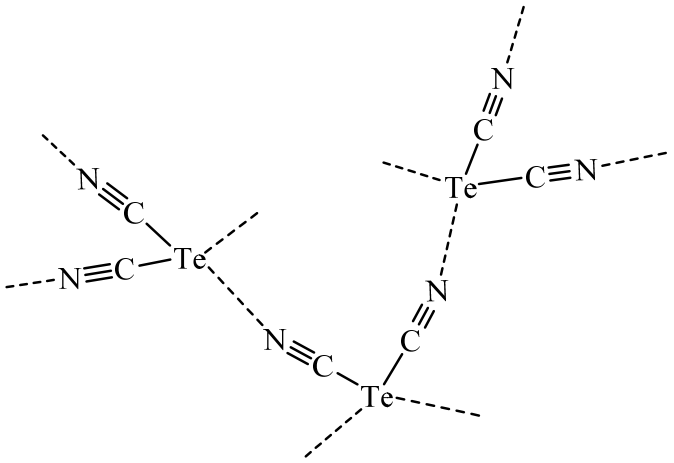

7

In these three cases, the close contacts between a Group IV − VI atom and a cyano nitrogen did identify the Coulombic interactions that control the crystal structure. However there are other instances in which close contacts are not as successful.

One of these is 2-nitromethylene-1,3-dithietane, **8**. Its crystal lattice contains pairs of parallel chains of oppositely oriented molecules,[53] approximately as in structure **9**. Between the pairs of chains are hydrogen bonds involving nitromethylene hydrogens and nitro oxygens. There are also two sets of intermolecular S---O close contacts, 2.900 Å and 3.077 Å, which are well below the sum of the sulfur and oxygen van der Waals radii given by either Rowland and Taylor[11] or Alvarez[13], 3.4 Å. It was suggested that the formation of the chains could be attributed to interactions represented by these close contacts.[53] This would of course be consistent with S---O σ-hole bonds involving sulfur σ-holes on the extensions of the C-S bonds. The C-S---O angles are 162.75° and 167.85°.

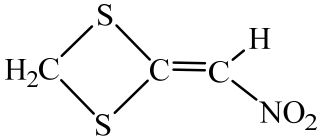

8

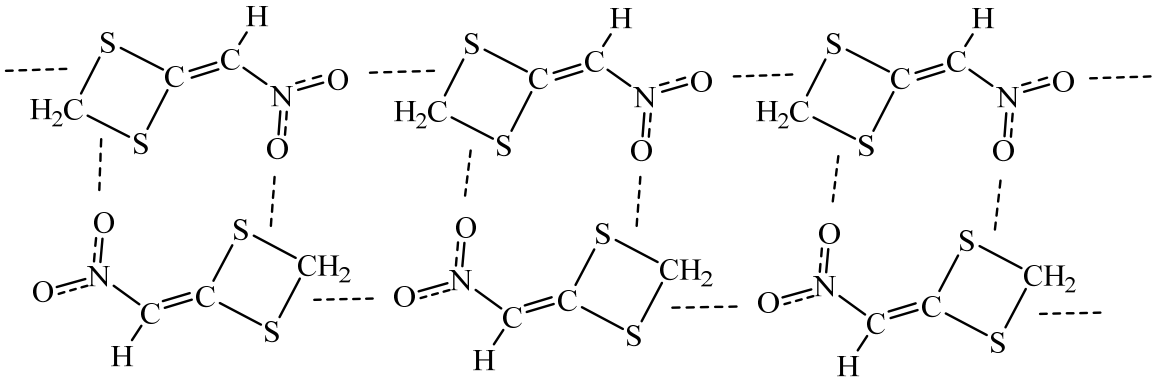

9

However crystal structure **9** also features C---O intermolecular close contacts within the chains, involving the same nitro oxygens as are in the S---O contacts. The C---O separations are 3.181 Å, again less than the sum of the van der Waals radii, 3.4 Å[11] or 3.3 Å.[13] These might be attributed to S-C---O bonding, involving carbon σ-holes on the extensions of the S-C bonds. The S-C---O angles are 157.69°, less than the C-S---O.

To try to clarify the nature of the intermolecular interactions in the crystal lattice **9**, we computed the electrostatic potential of **8** on its 0.001 au molecular surface. It is displayed in Figure 4. The strongest positive potentials are associated with the dithietane ring and with the CH_2 hydrogens, the latter being above and below the plane of the ring. The three positive regions in the plane of the dithietane ring have $V_{S,max}$ between 33 and 35 kcal/mol. However none of them can be described as being on the extension of either a C-S or an S-C bond; instead they are located *between* these extensions, deviating by 26° to 37° from the former and 18° to 28° from the latter. Thus the nitro oxygen of a neighboring molecule is not interacting directly with either a sulfur or a carbon σ-hole; its interaction is with the positive site that has developed between these σ-holes.

No fourth positive region is visible on the remaining side of the dithietane ring because it is interacting *intramolecularly* with a nitro oxygen. It was indeed reported that there is an

intramolecular S---O close contact of 2.687 Å; however the interaction is presumably again with the positive site between the sulfur and the carbon, not with either one of them alone.

The crystal structures of several other dithietanes[54-56] suggest interactions analogous to those described above, between negative sites and positive regions that are strongest *between* the extensions of the C-S and S-C bonds, so that the interaction cannot be attributed definitively to either the carbon or the sulfur. The presence of such positive regions was verified by electrostatic potential calculations in the case of tetrafluoro-1,3-dithietane, **10**.[56] The $V_{S,max}$ diverge from the extensions of the S-C and C-S bonds by 18° and 36°, respectively. This clearly puts the $V_{S,max}$ between the extensions of the bonds, not associated specifically with either the carbon or the sulfur.

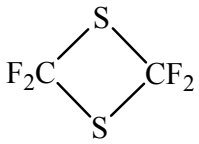

10

What is apparently occurring in these dithietanes is that the positive potentials expected for the separate carbon and sulfur σ-holes overlap and reinforce each other in the region between the extensions of the C-S and S-C bonds. This produces just a single $V_{S,max}$, located in that middle region. It is with this positive middle region that a negative site interacts, e.g. a fluorine on a neighboring molecule in crystalline **10**. The significance of this is that the interactions that control these dithietane crystal structures do not correspond to the crystallographically observed close contacts, which specify atoms and not regions.

To investigate this further, we considered first the analogue of **10** in which the four-membered ring is composed of atoms in the next row of the periodic table, structure **11**. The computed electrostatic potential on its molecular surface is displayed in Figure 5.

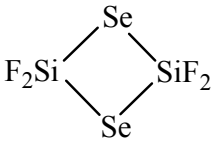

11

There are four strongly positive regions in the plane of the ring, with $V_{S,max}$ of 43 kcal/mol. However these do not follow the pattern of the dithietanes; the $V_{S,max}$ are not in the regions between the extensions of the Si-Se and Se-Si bonds, but instead are almost exactly on the latter! They are just 4^{o} from the extensions of the Se-Si bonds but 54^{o} from the extensions of the Si-Se bonds, and must be viewed as being associated specifically with the silicons. The selenium σ-holes do have positive potentials which overlap those of the silicon σ-holes, but the latter apparently determine the locations of the $V_{S,max}$. In the crystal lattice of **11**, therefore, Si---F close contacts would indeed correspond to the controlling interactions.

We looked at another four-membered ring that contains atoms of two different rows of the periodic table, structure **12**. The ring is now puckered rather than planar. Figure 6 shows the computed electrostatic potential on the molecular surface. This shows the dithietane pattern, with $V_{S,max}$ being between the extensions of the Se-P and P-Se bonds. Their magnitudes are 28 and 34 kcal/mol; the angles with the extensions of the Se-P bonds vary between 26^{o} and 31^{o} and the angles with the extensions of the P-Se bonds are between 38^{o} and 44^{o}. These $V_{S,max}$ cannot be attributed specifically to either the phosphorus or the selenium atoms.

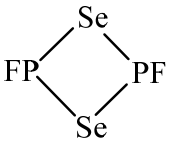

12

A further interesting feature of Figure 6 is related to the negative regions. While the fluorines and the selenium lone pairs have negative potentials, as expected, the phosphorus surface is completely positive; this even includes its lone pair.

We have also studied a five-membered heterocyclic ring, octafluorothiophane, **13**. The electrostatic potential on its molecular surface, Figure 7, features two strongly positive regions above and below the ring, with $V_{S,max}$ of 41 kcal/mol, and five positive regions that are in the plane of the ring. All five are essentially on the extensions of C-C or S-C bonds, within $2^o - 5^o$ of these extensions. What is particularly interesting is that three of these $V_{S,max}$ are simultaneously on the extensions of two different bonds. The $V_{S,max}$ on the extension of the S-C(2) is also on the extension of the C(4)-C(3); the one on the extension of the C(2)-C(3) is on the extension of the C(5)-C(4), and that on the extension of the C(3)-C(4) is on the extension of the S-C(5). These $V_{S,max}$, which have magnitudes of about 31 kcal/mol, are located at the points where the respective bond extensions cross. Each of them can be viewed as associated with two carbon σ-holes.

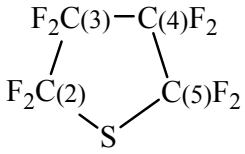

13

The two remaining $V_{S,max}$ in the plane of the ring are 35 kcal/mole and are on the extensions of the C(3)-C(2) and C(4)-C(5) bonds to within 4^o. However they deviate from the extensions of the C(2)-S and C(5)-S bonds by 22^o. The positive potentials of the carbon σ-holes seem to determine the locations of the $V_{S,max}$, but there is undoubtedly some overlap with positive regions of sulfur σ-holes on the extensions of the C(2)-S and C(5)-S bonds and the latter do have some effect.

This was brought out by interacting **13** with HCN as shown in **14**. Initially the HCN was set to be collinear with the C(4)-C(5) bond, as might be anticipated if the interaction involved just the

nitrogen lone pair of HCN and the positive σ-hole on the extension of the C(4)-C(5) bond,, where the $V_{S,max}$ is 35 kcal/mol. During the geometry optimization process, however, the HCN rotated until it was pointing approximately toward the middle of the C(5)-S bond. In the equilibrium geometry, the C(4)-C(5)---N angle is 176°, the C(2)-S---N is 166°. This suggests some interaction with the positive region of the sulfur. The binding energy of the complex, at the M06-2X/6-311G(d) computational level, was 12 kcal/mol.

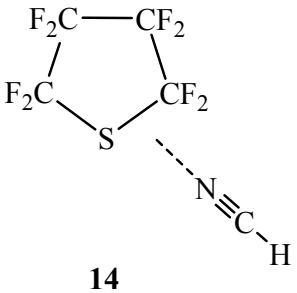

14

Our final case study is a hydrogen-bonded system, crystalline 1,3-dimethylurea, which has the molecular structure **15**. The crystal lattice is composed of chains of molecules with each oxygen having two O---H-N close contacts,[57] which were described as bifurcated hydrogen bonds. This is depicted in **16**. However the electrostatic potential on the molecular surface of **15** suggests a different interpretation. (It was computed using the molecular geometry of polymorph II in the crystal. In both polymorphs, the non-hydrogen atoms are coplanar, in contrast to the slightly puckered computed gas phase geometry.) The electrostatic potential, Figure 8, shows that the positive regions of the two N-H hydrogen σ-holes overlap and produce a single intermediately-located $V_{S,max}$ of 49 kcal/mol. The most negative potential of the carbonyl oxygen, −52 kcal/mol, is also in the middle of its negative region. Accordingly the more realistic way to describe the intermolecular interactions in the crystal lattice is structure **17**. The close contacts do not correspond to the dominant interactions. Analogous situations have been found in other hydrogen-bonded systems as well, e.g. due to overlapping of N-H hydrogen positive potentials in substituted ureas or of NO_2 oxygen negative regions in nitroaromatics.[58,59]

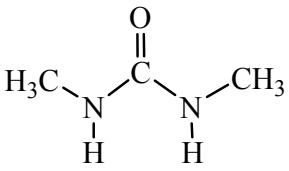

15

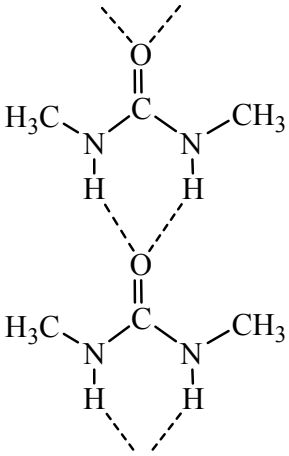

16

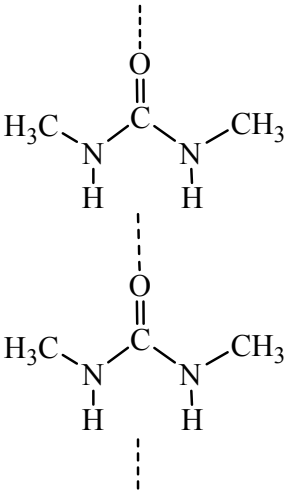

17

5. Discussion and Summary

Our concern in this paper has been the interactions that control the lattice structures of molecular crystals. Traditionally, these interactions have usually been interpreted in terms of observed intermolecular close contacts, i.e. pairs of atoms separated by less than the sum of their respective van der Waals radii. However we have shown that close contacts do not necessarily indicate the primary interactions. Proximity is a consequence but not an explanation of attractive interaction. The explanation is given by the Hellmann-Feynman theorem.

This theorem was derived by five different persons, [60-64] of whom Schrödinger was the first and Feynman the last. But it was Feynman who pointed out that the theorem shows rigorously

that both intra- and intermolecular interactions are purely Coulombic. This conclusion, which must be understood to include polarization and dispersion as well as static charge distributions, follows directly from the fact that the potential energy terms in the Hamiltonian operator are all Coulombic. (Charge transfer is sometimes invoked as an additional factor, but it is increasingly recognized that charge transfer, in noncovalent interactions, is just a mathematical representation of the actual physical effect, which is polarization.[65-72])

The forces that govern the lattice structures of molecular crystals are accordingly the Coulombic interactions between regions of positive and negative charge. The strongest such regions can be identified and located by means of the molecules' electrostatic potentials, keeping in mind that these may be modified by polarization.[30,71-73] The electrostatic potential is a real physical property, an "observable," which can be determined experimentally by diffraction methods[74-76] as well as computationally. (The electrostatic potential should not be confused with partial atomic charges, which are not observables, have no rigorous physical basis and cannot be measured experimentally.[77,78])

The strongest intermolecular Coulombic interactions within a crystal lattice do frequently correspond to crystallographic close contacts. As the preceding discussion has shown, however, this is not necessarily the case. The strongest positive and/or negative regions may not correspond to the positions of atoms; they may be located between these positions. For Group IV – VI atoms, in the absence of appropriate symmetry, the most positive regions are likely to deviate, sometimes considerably, from the extensions of the bonds to these atoms. By the Hellmann-Feynman theorem, it is the Coulombic interactions and hence the distribution of positive and negative charges, reflected in the molecular electrostatic potentials, that control the lattice structures. Note, in the examples that have been discussed, that when the strongest positive potential deviated from the extension(s) of the bond(s) that gave rise to σ-hole(s), the direction of the interaction with a negative site deviated in similar fashion.

In summary, close contacts in crystal lattices are certainly a very useful initial guide to the attractive interactions that are present. However they are not necessarily conclusive. The strengths and locations of positive and negative regions are the key.

References

1. P. Murray-Rust and W. D. S. Motherwell, *J. Am. Chem. Soc.*, 1979, **101**, 4374.
2. P. Murray-Rust, W. C. Stallings, C. T. Monti, R. K. Preston and J. P. Glusker, *J. Am. Chem. Soc.*, 1983, **105**, 3206.
3. N. Ramasubbu, R. Parthasarathy and P. Murray-Rust, *J. Am. Chem. Soc.*, 1986, **108**, 4308.
4. R. E. Rosenfield, Jr., R. Parthasarathy and J. D. Dunitz, *J. Am. Chem. Soc., 1977*, **99**, 4860.
5. T. N. Guru Row and R. Parthasarathy, *J. Am. Chem. Soc.*, 1981, **103**, 477.
6. N. Ramasubbu and R. Parthasarathy, *Phosphorus Sulfur*, 1987, **31**, 221.
7. P. Politzer, J. S. Murray, G. V. Janjič and S. D. Zarič, *Crystals*, 2014, **4**, 12.
8. L. Pauling, *The Nature of the Chemical Bond*, 3rd ed., Cornell University Press, Ithaca, NY, 1960.
9. A. Bondi, *J. Phys. Chem.*, 1964, **68**, 441.
10. S. C. Nyburg and C. H. Faerman, *Acta Cryst.*, 1985, **B41**, 274.
11. F. S. Rowland and R Taylor, *J. Phys. Chem.*, 1996, **100**, 7384.
12. I. Dance, *New J. Chem.*, 2003, **27**, 22.
13. S. Alvarez, *Dalton Trans.*, 2013, **42**, 8617.
14. T. Brinck, J. S. Murray and P. Politzer, *Int. J. Quantum Chem.*, 1992, **44**(Suppl. 19), 57.
15. T. Brinck, J. S. Murray and P. Politzer, *Int. J. Quantum Chem.*, 1993, **48**(Suppl. 20), 73.
16. E. D. Stevens, *Mol. Phys.*, 1979, **37**, 27.
17. S. L. Price, A. J. Stone, J. Lucas, F. S. Rowland and A. E. Thornley, *J. Am. Chem.Soc.*, 1994, **116**, 4910.
18. F. F. Awwadi, R. D. Willett, K. A. Peterson and B. Twamley, *Chem. Eur. J.*, 2006, **12**, 8952.
19. E. Bilewicz, A. J. Rybarczyk-Pirek, A. T. Dubis and S. J. Grabowski, *J. Mol. Struct.*, 2007, **829**, 208.
20. P. Politzer, K. E. Riley, F. A. Bulat and J. S. Murray, *Comput. Theor. Chem.*, 2012, **998**, 2.

21. M. S. Pavan, R. Pal, K. Nagarajan and T. N. Guru Row, *Cryst. Growth Des.*, 2014, **14**, 5477.
22. P. Politzer, J. S. Murray and T. Clark, *Phys. Chem. Chem. Phys.*, 2013, **15**, 11178.
23. T. Clark, M. Hennemann, J. S. Murray and P. Politzer, *J. Mol. Model.*, 2007, **13**, 291.
24. P. Politzer, J. S. Murray and T. Clark, *Phys. Chem. Chem. Phys.*, 2010, **12**, 7748.
25. D. Chopra and T. N. Guru Row, *CrystEngComm*, 2011, **13**, 2175.
26. P. Metrangolo, J. S. Murray, T. Pilati, P. Politzer, G. Resnati and G. Terraneo, *CrystEngComm*, 2011, **13**, 6593.
27. P. Metrangolo, J. S. Murray, T. Pilati, P. Politzer, G. Resnati and G. Terraneo, *Cryst. Growth Des.*, 2011, **11**, 4238.
28. V. R. Hathwar, D. Chopra, P. Panini and T. N. Guru Row, *Cryst. Growth Des.*, 2014, **14**, 5366.
29. J. S. Murray, K. E. Riley, P. Politzer and T. Clark, *Aust. J. Chem.*, 2010, **63**, 1598.
30. M. Hennemann, J. S. Murray, P. Politzer, K. E. Riley and T. Clark, *J. Mol.Model.*, 2012, **18**, 2461.
31. P. Politzer, J. S. Murray and T. Clark, *Top. Curr. Chem.*, 2015, **358**, 19.
32. Z. P. Shields, J. S. Murray and P. Politzer, *Int. J. Quantum Chem.*, 2010, **110**, 2823.
33. A. C. Legon, *Angew. Chem. Int. Ed.*, 1999, **38**, 2686.
34. A. C. Legon, *Phys. Chem. Chem. Phys.*, 2010, **12**, 7736.
35. R. F. W. Bader, M. T. Carroll, J. R. Cheeseman and C. Chang, *J. Am. Chem. Soc.*, 1987, **109**, 7968.
36. F. A. Bulat, A. Toro-Labbé, T. Brinck, J. S. Murray and P. Politzer, *J. Mol. Model.*, 2010, **16**, 1679.
37. S. C. Nyburg and C. H. Faerman, *Acta Cryst.*, 1985, **B41**, 274.
38. P. Politzer, K. E. Riley, F. A. Bulat and J. S. Murray, *Comput. Theoret. Chem.*, 2012, **998**, 2.
39. P. Politzer and J. S. Murray, in *Reviews in Computational Chemistry*, vol. 2, eds. K. B. Lipkowitz and D. B. Boyd, VCH Publishers, New York, 1991, ch. 7, pp. 273-312.
40. S. E. Wheeler and K. N. Houk, *J. Chem. Theory Comput.*, 2009, **5**, 2301.
41. J. S. Murray, Z. P.-I. Shields, P. G. Seybold and P. Politzer, *J. Comput. Sci.*, 2015, **10**, 209.

42. J. S. Murray, P. Lane and P. Politzer, *J. Mol. Model.*, 2009, **15**, 723.
43. A. Bundhun, M. D. Ramdany, J. S. Murray and P. Ramasami, *Struct. Chem.*, 2013, **24**, 2047.
44. P. Gagnaux and B. P. Susz, *Helv. Chim. Acta*, 1960, **43**, 948.
45. T. Bjorvatten and O. Hassel, *Acta Chem. Scand.*, 1961, **15**, 1429.
46. H. Hope and J. D. McCullough, *Acta Cryst.*, 1964, **17**, 712.
47. T. Dahl and O. Hassel, *Acta Chem. Scand.*, 1966, **20**, 2009.
48. H. A. Bent, *Chem. Rev.*, 1968, **68**, 587.
49. K. Olie and F. C. Mijlhoff, *Acta Cryst.*, 1969, **B25**, 974.
50. N. Camerman and J. Trotter, *Can. J. Chem.*, 1963, **41**, 460.
51. E. O. Schlemper and D. Britton, *Inorg. Chem.*, 1966, **5**, 511.
52. T. M. Klapötke, B. Krumm, J. C. Gálvez-Ruiz, H. Nöth and I. Schwab, *Eur. J. Inorg. Chem.*, 2004, 4764.
53. S. S. S. Raj, H. S. P. Rao, L. Sakthikumar and H.-K. Fun, *Acta Cryst.*, 2000, **C56**, 1113.
54. N. Kuhn, A. Al-Sheikh, C. Maichle-Mössmer, M. Steimann and M. Ströbele, *Z. Anorg. Allg. Chem.*, 2004, **630**, 1659.
55. V. A. Petrov, A. Marchione and W. Marshall, *J. Fluorine Chem.*, 2008, **129**, 1011.
56. S. K. Nayak, V. Kumar, P. Metrangolo, J. S. Murray, P. Politzer, T. Pilati, G. Resnati and G. Terraneo, *CrystEngComm*, 2017, in press.
57. C. Näther, C. Döring, I. Jess, P. G. Jones and C. Taouss, *Acta Cryst.*, 2013, **B69**, 70.
58. J. S. Murray, M. E. Grice, P. Politzer and M. C. Etter, *Mol. Eng.*, 1991, **1**, 75.
59. P. Politzer and J. S. Murray, *Cryst. Growth Des.*, 2015, **15**, 3767.
60. E. Schrödinger, *Ann. Phys.*, 1926, **80**, 437.
61. P. Güttinger, *Z. Phys.*, 1932, **73**, 169.
62. H. Hellmann, *Z. Phys.*, 1933, **85**, 180.
63. W. Pauli, *Handbuch der Physik*, 24. Springer, Berlin, p. 162.
64. R. P. Feynman, *Phys. Rev.*, 1939, **56**, 340.
65. K. Morokuma and K. Kitaura, in *Chemical Applications of Atomic and Molecular Electrostatic Potentials*, eds. P. Politzer and D. G. Truhlar, Plenum, New York, 1981, ch. 10, pp. 215-242.
66. A. E. Reed, L. A. Curtiss and F. Weinhold, *Chem. Rev.*, 1988, **88**, 899.

67. W. A. Sokalski and S. M. Roszak, *J. Mol. Struct. (Theochem)*, 1991, **234**, 387.
68. S. Scheiner, in *Reviews in Computational Chemistry*, vol. 2, eds. K. B. Lipkowitz and D. B. Boyd, VCH, Weinheim, 1991, ch. 5, pp. 165-218.
69. A. J. Stone and A. J. Misquitta, *Chem. Phys. Lett.*, 2009, **473**, 201.
70. R. J. Azar, P. R. Horn, E. J. Sundstrom and M. Head-Gordon, *J. Chem. Phys.*, 2013, **138**, 84102.
71. P. Politzer, J. S. Murray and T. Clark, *J. Mol. Model.*, 2015, **21**, 52(1-10).
72. P. Politzer and J. S. Murray, in *Noncovalent Forces*, S. Scheiner, ed., Springer, Heidelberg, 2015, ch. 10, pp. 291-321.
73. T. Clark, P. Politzer and J. S. Murray, *WIREs Comput. Mol. Sci.*, 2015, **5**, 169.
74. R. F. Stewart, *Chem. Phys. Lett.*, 1979, **65**, 335.
75. P. Politzer and D. G. Truhlar, eds., *Chemical Applications of Atomic and Molecular Electrostatic Potentials*, Plenum, New York, 1981.
76. C. L. Klein and E. D. Stevens, in *Structure and Reactivity*, J. F. Liebman and A. Greenberg, eds., VCH, New York, 1988, ch. 2, pp. 25-64.
77. S. L. Price, *J. Chem. Soc., Faraday Trans.*, 1996, **92**, 2997.
78. J. S. Murray and P. Politzer, *WIREs Comput. Mol. Sci.*, 2011, **1**, 153.

Figure Captions.

Figure 1. Computed electrostatic potential on the 0.001 au molecular surface of 4-bromo-2*H*-1,2,3-triazole, **1**. Gray circles correspond to positions of atoms. Bromine is at lower left, N-H is at right. Color ranges, in kcal/mol: red, greater than 22; yellow, between 22 and 11; green, between 11 and 0; blue, less than 0 (negative). Black hemispheres indicate locations of the $V_{S,max}$ of the positive potentials corresponding to the σ-holes on the extensions of the N-H, C-H and C-Br bonds.

Figure 2. Computed electrostatic potential on the 0.001 au molecular surface of cyanodimethylarsine, **2**. Color ranges, in kcal/mol: red, greater than 18; yellow, between 18 and 10; green, between 10 and 0; blue, less than 0 (negative). In (a), two methyl groups are in the foreground, the arsenic is in the center and its lone pair is at the top. Black hemisphere indicates $V_{S,max}$ of positive region formed by overlapping of potential of σ-hole on extension of NC-As bond with those due to C-H bonds of two methyl hydrogens. In (b), two methyl groups are at lower left and lower right, the arsenic lone pair is in the center and the lone pair of the cyano nitrogen is at the top. Black hemispheres show locations of $V_{S,max}$ of σ-holes potentials on extensions of H_3C-As bonds.

Figure 3. Computed electrostatic potential on the 0.001 au molecular surface of cyanotrimethylgermane, **3**. Color ranges, in kcal/mol: red, greater than 18; yellow, between 18 and 10; green, between 10 and 0; blue, less than 0 (negative). In (a), methyl groups are in foreground. Black hemisphere indicates $V_{S,max}$ for σ-hole on extension of NC-Ge bond. In (b), lone pair of cyano nitrogen is at top, methyl groups at bottom. Black hemispheres correspond to $V_{S,max}$ of σ-hole potentials on extensions of H_3C-Ge bonds.

Figure 4. Computed electrostatic potential on the 0.001 au molecular surface of 2-nitromethylene-1,3-dithietane, **8**. Gray circles correspond to positions of atoms. CH_2 of the four-membered ring is at lower left, nitromethylene group is at right. Color ranges, in kcal/mol: red, greater than 28; yellow, between 28 and 0; green, between 0 and -20; blue, more negative than -20. Black hemispheres show locations of $V_{S,max}$ in the plane of the ring; all three are between the extensions of the C-S and S-C bonds.

Figure 5. Computed electrostatic potential on the 0.001 au molecular surface of structure **11**. Gray circles show positions of the atoms of the four-membered ring. The seleniums are at the

top and bottom. Color ranges, in kcal/mol: red, greater than 24; yellow, between 24 and 12; green, between 12 and 0; blue, less than 0 (negative). There are four $V_{S,max}$ in the plane of the ring; two of them can be seen, indicated by black hemispheres. All four are on the extensions of Se-Si bonds and correspond to silicon σ-holes.

Figure 6. Computed electrostatic potential on the 0.001 au molecular surface of structure **12**. gray circles show positions of the atoms of the four-membered ring. The seleniums are at the top and bottom. Color ranges, in kcal/mol: red, greater than 20; yellow, between 20 and 10; green, between 10 and 0; blue, less than 0 (negative). Black hemispheres indicate locations of $V_{S,max}$ in the plane of the ring; all four are between the extensions of the Se-P and P-Se bonds.

Figure 7. Computed electrostatic potential on the 0.001 au molecular surface of octafluorothiophane, **13**. Gray circles show positions of the atoms of the five-membered ring. Color ranges, in kcal/mol: red, greater than 20; yellow, between 20 and 10; green, between 10 and 0; blue, less than 0 (negative). View (a) shows the entire ring; the sulfur is at the bottom. The upper black hemisphere corresponds to a $V_{S,max}$ above (below) the ring. The two lower ones are on the extensions of the C(3)-C(2) and C(4)-C(5) bonds and correspond to carbon σ-holes. Part (b) is a side view of the ring; the black hemispheres show the locations of three $V_{S,max}$ that are simultaneously on the extensions of two C-C bonds. Each of these $V_{S,max}$ is associated with two carbon σ-holes.

Figure 8. Computed electrostatic potential on the 0.001 au molecular surface of 1,3-dimethylurea, **15**. Gray circles show positions of the atoms. Color ranges, in kcal/mol: red, greater than 30; yellow, between 30 and 0; green, between 0 and -20; blue, more negative than -20. The black hemisphere shows the location of the $V_{S,max}$ that results from the overlap of the positive potentials of the σ-holes of the two N-H hydrogens.

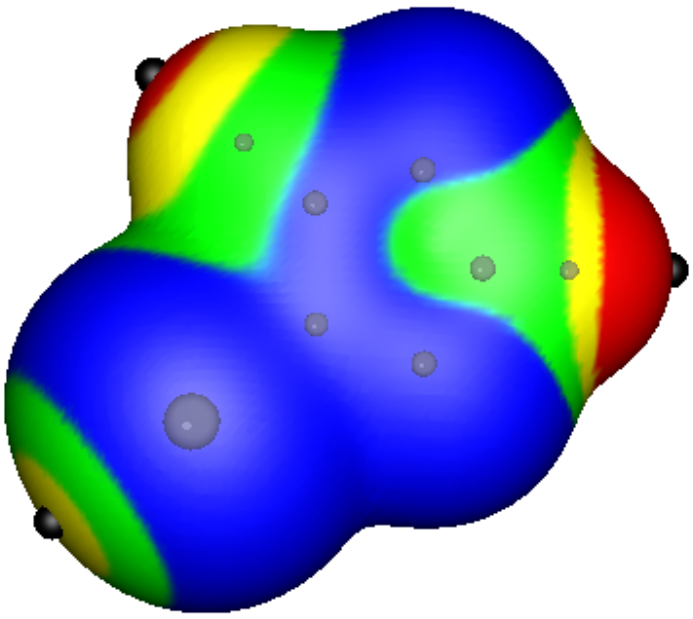

Figure 1.

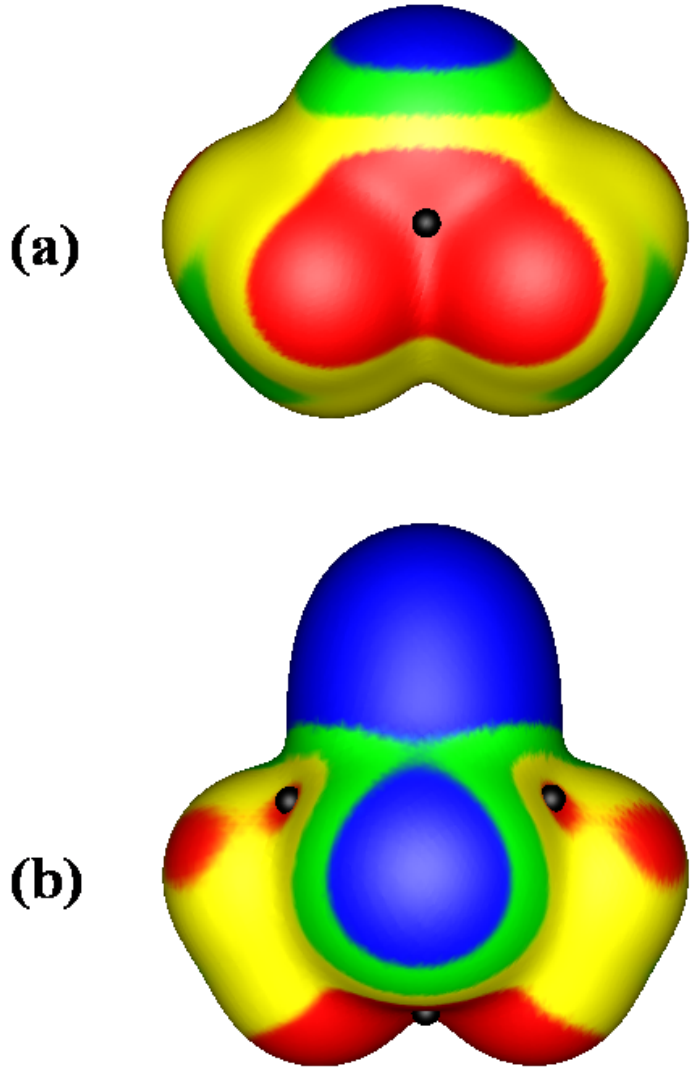

Figure 2.

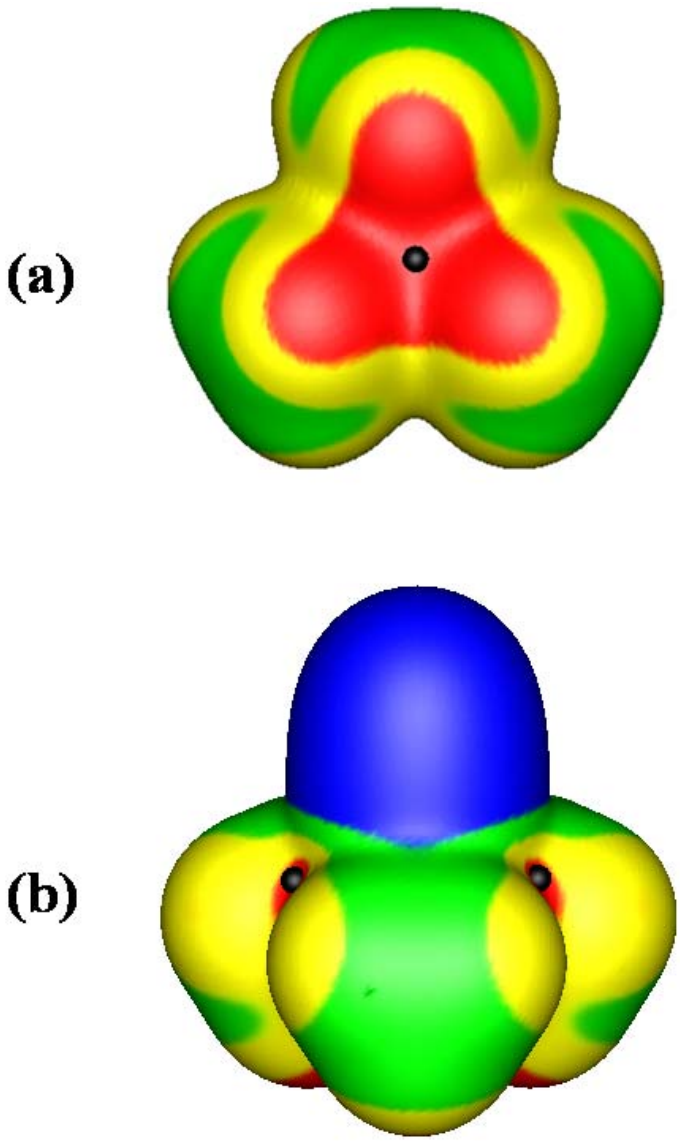

Figure 3.

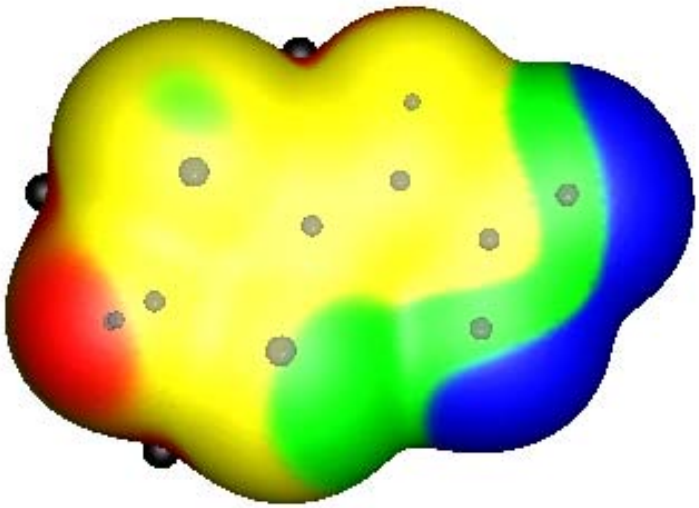

Figure 4.

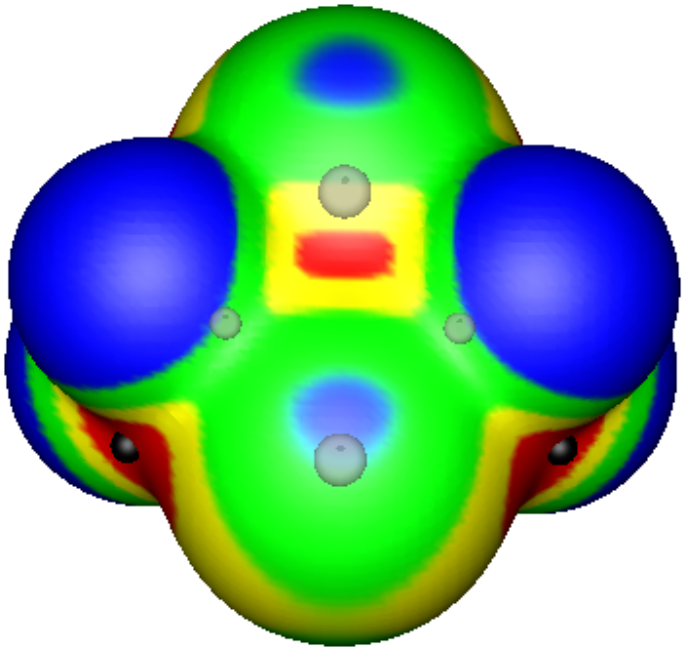

Figure 5.

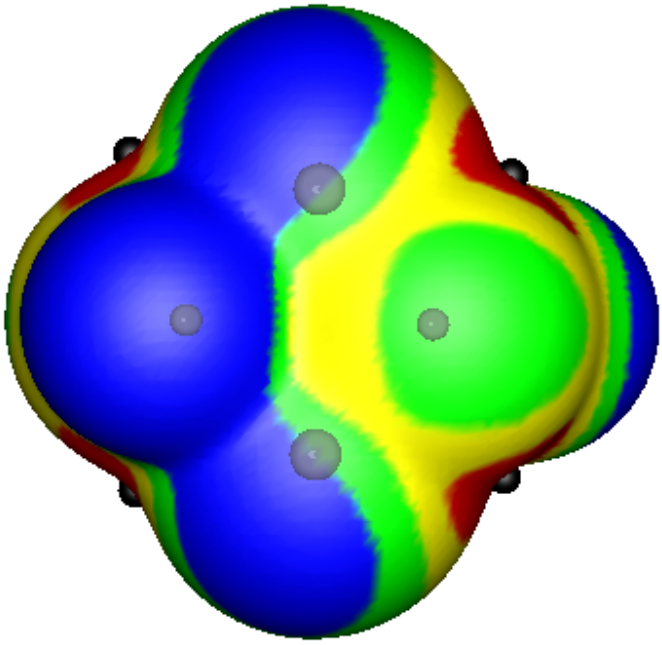

Figure 6.

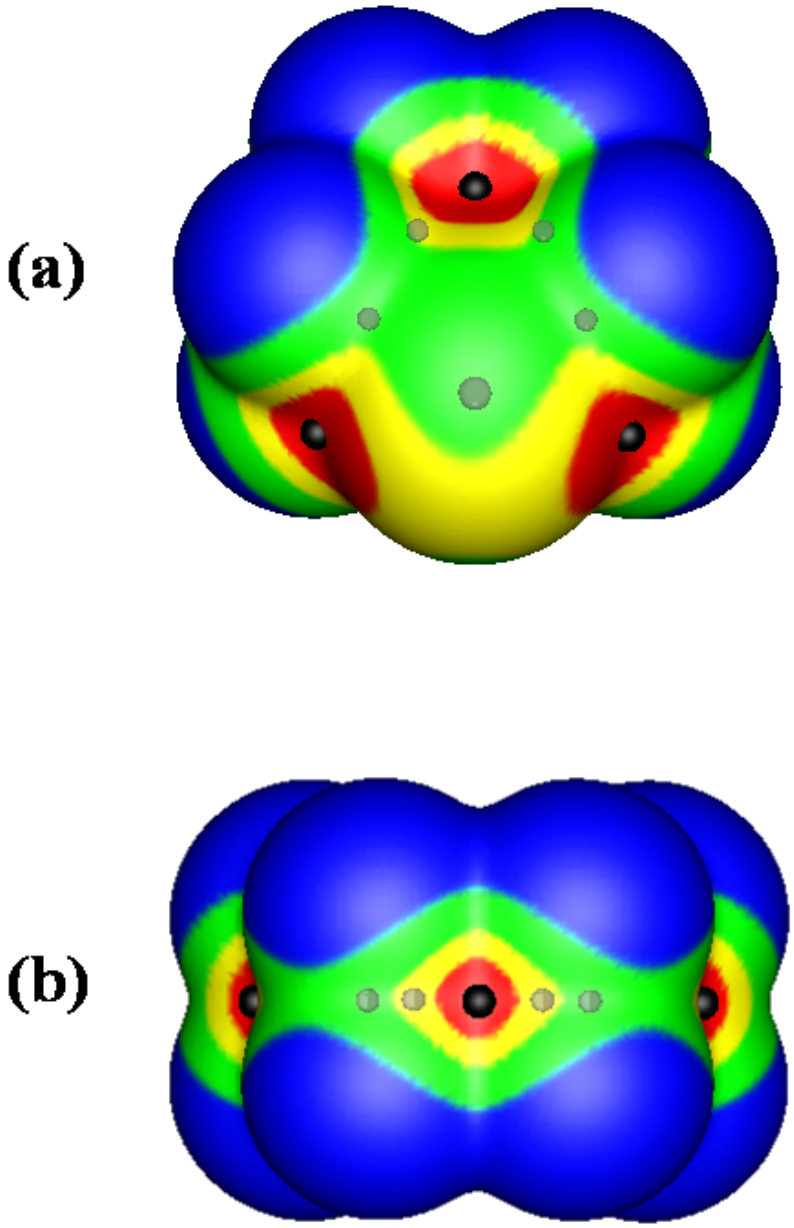

Figure 7.

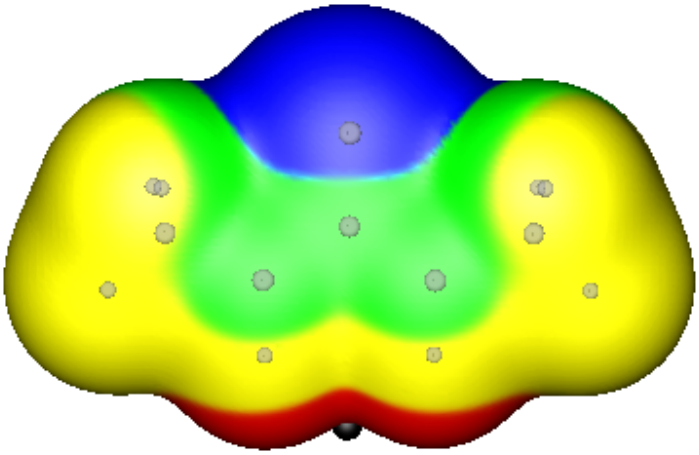

Figure 8.